Appl. Phys. B 78, 995–1000 (2004)
DOI: 10.1007/s00340-004-1449-y

Applied Physics B
Lasers and Optics

T.E. GLOVER[1,✉]
G.D. ACKERMAN[1]
R.W. LEE[2]
D.A. YOUNG[2]

Probing particle synthesis during femtosecond laser ablation: initial phase transition kinetics

[1] Advanced Light Source Division, Lawrence Berkeley National Laboratory, Berkeley, California 94720, USA
[2] Physics Department, Lawrence Livermore National Laboratory, Livermore, California 94550, USA

Received: 31 October 2003/Revised version: 9 January 2004
Published online: 7 April 2004 •

ABSTRACT The impulsive superheating of matter by an intense, ultrashort laser pulse drives material expansion into vacuum (ablation) and an associated formation of nanoparticles. The underlying dynamics of particle formation are complex and direct experimental probes of the rapid material evolution are essential. Femtosecond lasers coupled to modern synchrotrons offer an important new opportunity to probe ejecta dynamics on an atomic lengthscale. Here, the impulsive heating of a semiconductor (silicon) by an intense femtosecond laser pulse leads to material ejection and time-resolved photoemission spectroscopy probes rapid solidification kinetics occurring within the ejecta. Transient photoemission peak-shifts indicate that material is ejected predominantly as liquid droplets and that solidification occurs rapidly (< 50 ps). The solidification time suggests that vacuum ejection leads to significantly enhanced undercooling compared to what has been obtained by more conventional quenching techniques; this may be of interest in attempts to 'trap' novel material states associated with extreme laser heating. Finally, a low fraction of vapor particles in the ejecta supports a view that the size-distribution of ejected particles is set by an initial fragmentation process rather than by vapor condensation.

PACS 82.60.Qr; 87.64.Lg; 62.50.+p

1 Introduction

In laser ablation a material is rapidly heated to a point where the system's thermal energy exceeds its cohesive energy; material ejection occurs leading to rapid cooling and an associated synthesis of particles. This process is of considerable practical importance since ablation is used to synthesize organic and inorganic nanoparticles, microparticles and films [1–3]. As a nanoparticle synthesis technology, ablation is attractive since it is easily applied to a range of materials and since initial laser-heating to extreme temperature may produce novel material states which, in turn, may survive if they can be trapped by rapid quenching. While hydrodynamic estimates indicate that very high quench rates ($> 10^{15}$ K/s [4]) are possible from vacuum expansion, hydrodynamic (i.e. continuum) models average away information on atomic lengthscales and are therefore of limited use in predicting the kinetics by which nanoparticles form during shortpulse laser ablation. Direct experimental probes of the rapid phase transition kinetics are essential.

Experimentally, it has proven difficult to directly probe transient material properties in the early moments of vacuum expansion. Material is only a few microns from the bulk surface so absorption/reflection spectroscopes interact with the residual surface and do not distinguish surface-dynamics from ejected-material dynamics. Time-resolved photoemission spectroscopy is well suited to probing the early moments of vacuum expansion: one probes solely the ejecta since the photoemission probe depth is set by the electron escape depth ($<\sim 1$ nm [5]) which is short compared to typical ablation depths (> 10 nm [6]). Further, core-level photoemission spectroscopy (CPS) is a local probe well known for providing chemical sensitivity [5]; one may therefore follow the evolving chemical state of ejected material. To date CPS has primarily probed static chemical properties. Here CPS is extended to the picosecond time domain to probe the early-time kinetics through which solid-phase particles form during the vacuum expansion of an impulsively superheated semiconductor (silicon).

The very earliest moments of lattice heating and vacuum expansion are inaccessible owing to finite time resolution and future femtosecond-time-resolved experiments are required to answer an interesting question: can second-order metal–insulator transitions be observed as the ejecta passes near the liquid–vapor critical point (discussed below)? The current experiments are sensitive to metal–insulator transitions occurring on a tens-of-picoseconds timescale; in this regime one probes first-order metal–insulator transitions which reflect the chemical evolution of the ejecta. The observed photoemission peak-shifts reveal rapid metal–insulator transitions and provide insight into transient chemical properties of the ejecta. The present analysis extends beyond that discussed in a recent letter [7] to address an issue relevant in attempts to trap possibly novel material states via rapid quenching: we estimate the degree of undercooling as ejecta solidify following vacuum ejection. The undercooling is estimated in two ways: 1) a realistic equation-of-state for silicon is coupled to hydrodynamic simulations to estimate the degree of undercooling at the measured solidification time and 2) the degree of undercooling is estimated from the experimental (solidification) nu-

✉ Fax: +1-510/486-5530, E-mail: teglover@lbl.gov.

cleation rate. We find that undercooling associated with vacuum expansion is significantly enhanced compared to what has been obtained by more conventional quench techniques. Vacuum expansion, therefore, is an attractive route in attempts to trap potentially novel material states produced by extreme laser heating. Finally, a low fraction of vapor particles in the ejecta supports a view that the size-distribution of ejected particles is set by an initial fragmentation process rather than by vapor condensation. These experiments demonstrate an ability to probe constituent species and solidification kinetics occurring early in the vacuum expansion of an extreme material and provide insight into how particles arise in the current laser ablation regime.

2 Experiment & data

The experimental arrangement has been discussed previosuly [7]. Briefly, laser-pump and X-ray-probe photoemission experiments are performed at the Advanced Light Source (ALS) using a laser system (800 nm, 200 fs, 1 kHz) synchronized to the ALS storage ring.. A femtosecond laser pulse ($4–12\,\mathrm{J/cm^2}$) excites a thin surface layer of a silicon wafer to extreme temperature and pressure (estimated at $\sim 20\,000$ K and 14 GPa) producing a highly pressurized and likely supercritical ($T_{\mathrm{critical}} \sim 5000$ K) fluid which expands into vacuum. Vacuum expansion is probed by time-delayed synchrotron pulses (80 ps, 400 eV) with X-ray photoelectrons in the vicinity of the Si $2p$ core-level collected using a hemispherical analyzer. Measurements at a fixed pump–probe delay reflect the spectral evolution over a time-window set by a single X-ray pulse (~ 80 ps). Photoemission transients lasting shorter than 80 ps can be observed although better noise statistics are required for shorter transients. Current noise levels (10–20%) allow one to see photoemission peak shifts lasting longer than $\sim 10–20$ ps (10–20% of 80 ps).

At the laser excitation rate of 1 kHz, a given sample region is exposed to multiple pump–probe cycles; the initial (unheated) material is therefore either micro-crystalline or amorphous. While we cannot discount that single-shot-heating of single-crystal-silicon would produce different results from those discussed below, we think it unlikely that the vacuum expansion dynamics would be different in any significant way for two reasons. First, the vacuum expansion is set by the temperature/pressure of the initial solid density fluid. Since the phase transformation parameters (heats of transformations etc. [8]) are similar between amorphous and crystalline silicon the initial parameters of the hot/pressurized fluid should be similar in the two cases. Second, static spectra show only a small ($<\sim 0.2$ eV) peak shift and no peak-shape-distortion between a 'fresh' silicon surface and a laser-exposed surface. Therefore, relative to the large (~ 1 eV) shifts discussed below, differences in even the solid-phase pristine vs. damaged sample-regions are modest.

A temporal sequence of X-ray photoelectron spectra is shown in Fig. 1 (inset) and indicates a transient photoelectron peak shift; an initial shift to lower binding energy (200 to 0 ps) following by a subsequent return back towards higher binding energy (0 to -160 ps). The timescale of the photoemission transient is determined by measuring electron counts in the vicinity of the spectral shift as a function of pump–probe delay. This measurement, a convolution of the X-ray pulse duration and the material transient timescale, is found to be resolution limited by the ALS pulse duration (80 ps) and from error bars on the correlation we place an upper limit of 50 ps on the timescale of the transient spectral modification. Significantly, since the spectrum is perturbed for a time (< 50 ps) less than the X-ray duration, a temporal deconvolution of the (perturbed) photoemission spectrum is necessary. This is to say that a (perturbed) spectrum at a fixed delay must contain at least two peaks: one corresponding to transiently perturbed material and another to unperturbed material (which, depending on delay, is either recovered or not yet excited). The temporal deconvolution is shown in Fig. 1 (main figure).

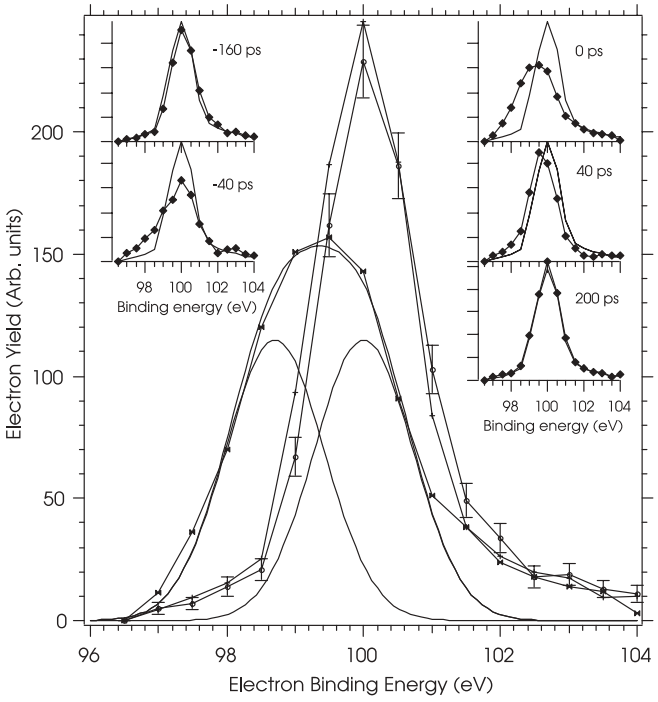

FIGURE 1 *Inset*: Temporal sequence of Si $2p$ photoemission spectra at specified pump–probe delays. Positive delay indicates that the X-rays probe before arrival of the laser pump. A reference spectrum at +240 ps is also shown (*dashed line*). *Main Figure*: Photoemission spectra when X-ray probes well before laser excitation (240 ps, *crosses*, 1.7 eV FWHM photoemission peak-width), well after laser excitation (-160 ps, *circles*, 1.7 eV peak-width), and simultaneous with laser excitation (0 ps, *bow-ties*, 2.7 eV peak-width). The broadened peak is decomposed into two Gaussians of width 1.7 eV: a 'perturbed' peak (*dashed curve* at 98.7 eV with amplitude 115) and an 'unperturbed' peak (100 eV with amplitude 115). The sum of these two Gaussians is also shown (*solid curve*)

Here spectra corresponding to X-ray probe times well before and well after laser excitation are shown (and are similar) while the spectrum corresponding to simultaneous arrival of X-ray and laser pulses is lowered, broadened, and shifted. The modified (i.e. perturbed) spectrum has been deconvolved assuming the simplest (i.e. two peak) deconvolution: one peak at the original position (unperturbed material) with the original width and a second peak of the same width but with adjustable position and height (perturbed material). A good fit to data is obtained for Gaussians of approximately equal amplitude and a photoelectron peak shift of ~ 1.3 eV. While better time and energy resolution are required to demonstrate the uniqueness

of this deconvolution, the shifted peak position is consistent with a fluid phase of silicon (discussed below).

As an additional point, the temporal deconvolution can be used to further specify the timescale of the transient material response. Specifically, the transient duration can be estimated since the ratio of shifted-to-unperturbed (deconvolved) peak amplitudes (Fig. 1) is approximately equal to the ratio of the X-ray pulse duration to the lifetime of the spectral transient (note that the shifted-peak amplitude will go to zero as material response becomes increasingly short compared to X-ray pulse duration). This ratio ($\sim 1/2$) indicates a transient duration of ~ 40 ps, consistent with the 50 ps upper limit discussed above. Finally, we mention that the total XPS yield is observed to be constant ($< 10\%$ variation).

3 Analysis

CPS probes the local state-of-aggregation through shifts in peak position which accompany a change in material phase. The observed spectral transient is consistent with a (transient) liquid phase of silicon. The current laser fluence exceeds the threshold fluence [9] for melting silicon so a fluid is produced following laser heating. To our knowledge calculations of the solid–fluid core-level peak shift in silicon are not available; relevant estimates, however, can be found for germanium [10]. Qualitatively, the solid–fluid transition in both silicon and germanium is an insulator (solid) to metal (fluid) transition [11]. An X-ray core-hole is more efficiently screened by the mobile electrons of a metal than by the immobile electrons of an insulator [5] and this difference in core-hole screening (extra-atomic relaxation) is the principle factor causing a peak shift to lower binding energy in the metal.

For a quantitative estimate there are three contributions to solid–fluid peak shift: (1) change in initial state energy, (2) change in final state energy (relaxation), and (3) possible change in surface potential (i.e. reference level [12]). Experiments and calculations on germanium indicate that final state (extra-atomic) relaxation dominates the solid–fluid shift; the K-absorption edge is observed to shift by 1.3–1.4 eV upon melting and changes in final state relaxation are calculated at ~ 1.2 eV [10]. We take this number (1.2 eV) as an estimate of the solid-fluid shift in silicon. In doing so we assume 1) that final state relaxation dominates in silicon as well as in germanium and 2) that final state relaxation is of comparable magnitude in silicon and germanium. The first assumption is reasonable for insulator–metal transitions since relaxation shifts can be large (~ 1 eV) while initial state modification should be comparatively small. Initial state modification reflects changes in the local potential due to neighbor atoms; the solid-atom shift in silicon (reflecting presence vs. absence of neighbors) has been calculated at ~ 1 eV [13]. The corresponding solid–fluid shift should be comparatively small since it results from the more modest rearrangement of neighbors. Similarly, the surface potential is small (~ 0.2 eV [14]) and possible solid–fluid variations are neglected. As for the second assumption, it is reasonable to assume that relaxation, reflecting the polarization energy between a core-hole and the induced charge distribution [5], is comparable in silicon and germanium. The metallic fluids have nearly identical carrier density (2×10^{23}/cc [11]) so the polarizabilities should be similar. Further, the solids have similar dielectric constants ($\varepsilon = 11.9$ for Si and $\varepsilon = 16$ for Ge [8]); the (macroscopic) polarization energy scales as $(1 - 1/\varepsilon)$ and this factor varies by $< 10\%$. While core-hole size differs in the Ge ($1s$) and Si ($2p$) cases, Bechstedt [15] calculates only modest changes in relaxation energy with hole-size ($< 10\%$ difference in moderately polarizable media between Si $1s$ and $2p$ holes). While detailed theoretical calculations from the community are strongly encouraged, the solid–fluid shift in Ge (1.2 eV) provides a reasonable estimate for the corresponding shift in silicon. Accordingly, the spectral transient of Fig. 1 reflects a solid–fluid–solid sequence of phase transitions: material first melts following laser heating; this should produce a solid-fluid shift of ~ 1.2 eV while we observe a ~ 1.3 eV shift (deconvolution Fig. 1). Subsequently, material re-solidifies after vacuum ejection (and associated cooling) and the photoemission peak returns to the position characteristic of solid silicon.

We emphasize that we are probing dynamics within the ejecta rather than at the bulk surface since both lattice heating and material ejection occur rapidly ($\ll 10$ ps); 80 ps probe pulses render us insensitive to these very earliest moments before material ejection. Similarly, after expulsion the ejecta shield the underlying bulk surface (electron escape depth short compared to ablation depth). Significantly, metallic core-hole screening (i.e. fluid Si) is observed to persist for < 50 ps and we take this as evidence that the ejected material has solidified on this rapid timescale; hydrodynamic simulations discussed below support the feasibility of such rapid solidification following vacuum ejection. Analysis of the time-dependent spectra therefore leads to the finding that material is ejected initially as a metallic fluid which then undergoes rapid (< 50 ps) solidification.

4 Discussion

4.1 *Ejecta composition and fragmentation*

Shortly following laser heating the initial fluid will expand into vacuum and one may pose a basic yet non-trivial question: what state-of-aggregation does expansion lead to? Is material ejected predominantly as single atoms with larger units formed subsequently by aggregation or is material initially ejected in larger units? Lattice heating in silicon occurs rapidly (~ 1 ps) so for high initial temperature atoms quickly have energy above the cohesive energy and are loosely speaking 'unbound'. Material will be ejected in vapor form if upon ejection the interatomic spacing is increased so that neighbor atom wavefunctions cease to overlap. A condensed phase is preserved if expansion is largely inhomogeneous, with the average density dropping but the local density remaining high.

This basic question about the ejecta phase is not easily answered. Extreme materials are often treated using continuum models which average away information on atomic length-scales; yet it is precisely the microscopic (local) expansion dynamics which determine the state-of-aggregation. Significantly, the current experiments provide insight into the critical local expansion dynamics. We find that spectral weight is conserved in the solid–fluid (transient) peak and this indicates that a condensed phase dominates the ejecta, a finding which is supported by a second feature of the data: we find

an absence of spectral weight at the vapor-phase position. The atom–solid peak shift can be estimated since estimates can be found for the initial state shift (~ 1.4 eV [13]), the change in (extra-atomic) relaxation (4.7 eV [15]), and the value of the surface potential (~ 0.2 eV [14]). Accordingly, vapor particles (isolated atoms) should be shifted ~ 3.5 eV to higher binding energy relative to the solid. Given the absence of spectral weight at this location and $\sim 10\%$ accuracy on the data we conclude that vapor particles comprise $< 10\%$ of the ejected material. Analysis of the time-dependent spectra therefore indicates that vapor particles comprise only a modest fraction of the ejecta. We make two comments with regard to this finding. First, it indicates that the current vacuum expansion is microscopically inhomogeneous. While the average density drops from vacuum expansion, a high local density is preserved so that wavefunction overlap is maintained and a vapor phase is largely suppressed. As mentioned above, this finding on a basic feature of the vacuum expansion process is not easy predicted since the continuum models often used for extreme materials average away the relevant local information.

Before continuing on to the second point, we briefly address an issue that has arisen in the context of a referee comment. Specifically, one may ask what affect does the drop in ejecta density have on the photoemission spectrum? A change in the ejecta density could be due to a change in the local density (i.e. distance between atoms), a change in (macroscopic) average density, or both. The possibility of an appreciable change in local density is precisely what was discussed in the preceding paragraph. A significant drop, for instance, would be observed as a photoemission peak shift to higher binding energy owing to modifications in local potential and local screening. Stated generally, changes in local density are observable as chemical shifts of the photoemission peak location. Next consider changes in the (macroscopic) average density. We will assume that the local density remains high since this is the case for our data (i.e. no appreciable vapor phase). We then imagine a fluid initially (i.e. before expansion) at solid density and we collect X-ray photoelectrons from the top ~ 1 nm of material. This means that an X-ray photoelectron has a high probability of passing by N atoms without suffering an energy-loss collision; N is equal to solid-density times 1 nm (considered in 1-D for simplicity). Next, consider a later time: material has expanded to reduce the average density and one can imagine a collection of fragments of local high density. The drop in average density has no observable affect on the spectrum. The photoelectron can pass by a given number of atoms and it does not matter whether the 'fragments' are compressed together (before expansion) or dispersed (after expansion). This is equivalent to saying that core-level photoemission is sensitive to the local density and that changes in macroscopic density are comparatively unimportant. To make one final point: if one waits a very long time then the ejecta would move far away from the underlying Si surface; X-rays would then strike the underlying surface rather than the ejecta and we would no longer be probing the ejecta. This never happens in the current (0–1 ns) experiment and we offer two supporting statements. First, the underlying silicon surface is known to stay molten for a time much longer than 1 ns [16]; the fact that we see rapid ($<$50 ps) solidification therefore supports a view that the ejecta shields the underlying surface. Second, the ejecta expansion velocity is estimated at $\sim 10\,\mu$m/ns; accordingly for all time delays the ejecta is very close to the underlying bulk and therefore shields the underlying bulk.

Next, as a second comment relevant to finding a small fraction of vapor particles, we note that this finding offers important insight into the underlying mechanisms of particle formation. The low fraction of vapor particles indicates that in contrast to longpulse ablation [17] particles do not arise by condensation of a dilute vapor. In longpulse ablation material is ejected into an intense laser field and it is likely that secondary laser–ejecta interactions (photo-fragmentation, collisional processes, etc.) contribute to the production of vapor particles. In shortpulse ablation secondary laser interactions are eliminated and this ensures that the nascent particle-size-distribution is determined by the vacuum expansion process. The sudden vacuum expansion of energetic matter is of interest to a number of scientific disciplines and simulations have established that strain associated with gradients in the local expansion velocity leads to material fracture and an associated size-distribution of 'fragments' [18, 19]. We therefore expect the nascent particle-size-distribution in shortpulse ablation to be determined primarily by an initial fragmentation process; recent simulations have probed the role of fragmentation in shortpulse ablation [19].

4.2 *Rapid solidification and undercooling*

Finally, we discuss the implications of rapid solidification. Rapid solidification suggests a highly non-equilibrium phase transition. (Quasi) equilibrium phase transitions occur via nucleation and growth [20]. We estimate that such a transition would take ~ 25 ns given the measured solidification interface velocity (25 nm/ns [21]) and estimates of our probe volume (10^9 nm^3) and size of a critical nucleus (~ 1 nm [20]). This time is nearly three orders of magnitude greater than the observed solidification time and suggests that the solid phase nucleates throughout a substantial fraction of the probe volume on a < 50 ps timescale. Phase transition by homogeneous nucleation (rather than by interface propagation) has been referred to as phase explosion [22] and signatures a highly undercooled material phase. Efficient undercooling may allow one to trap novel material states and we next estimate the degree of undercooling in two ways: 1) by hydrodynamic simulation and 2) through use of classical nucleation theory.

Hydrodynamic estimate of undercooling. As discussed above solidification is observed to occur ~ 40 ps after laser heating. We first estimate the degree of undercooling through hydrodynamic estimates of the ejected material temperature at 40 ps. We model the hydrodynamics using a similarity profile [23] coupled to a realistic equation-of-state for silicon (global equation-of-state model QEOS [24]). Since heat conduction is negligible during the initial moments of vacuum expansion we adopt the common assumption of isentropic vacuum expansion.

Before estimating the degree of undercooling associated with the observed first-order phase transition from liquid

droplets to solid particles, we discuss the timescale relevant for a possible second-order phase transition which could occur in the vicinity of the liquid–vapor critical point. Since a second-order phase transition would occur at much higher temperature (i.e. near the critical point) it will occur much more rapidly following laser excitation. We note that (second-order) metal–insulator phase transitions occurring in the vicinity of a critical point are of fundamental interest from the perspective of correlated-electron physics. Experimental study of these expanded liquid metals, however, has been severely hampered because the critical temperature/pressure of most materials is too high to access under steady state conditions. A transient laser heating technique is, therefore, of interest as a possible route for placing nearly any material (transiently) in the vicinity of a critical point. With adequate time resolution one may then probe possible metal–insulator transitions as the material rapidly evolves through phase space. Here we use the hydrodynamic simulations to estimate the required time-resolution. QEOS is used to calculate isentropes at initial lattice temperatures ranging from 1–5 eV (critical temperature for silicon ~ 5000 K, ~ 0.5 eV).The isentropes are then coupled to the hydrodynamic model to estimate the time to cool to the vicinity of the critical point. We find that material reaches the critical-point-vicinity after expanding into vacuum for a time on order of 1 ps. Further, that material cools at a rate exceeding 3000 K/ps and will therefore rapidly move through the critical-point-vicinity. Accordingly, subpicosecond time resolution is likely needed to view possible second-order phase transitions near a critical point. Owing to our finite time resolution we are sensitive to peak-shifts lasting longer than $\sim$ 10–20 ps. Accordingly we are insensitive to the very earliest moments of lattice heating and vacuum expansion; in particular, to any possible metal–insulator transitions near the critical point. Higher time resolution is required to assess whether or not these early-time phase transitions occur.

Instead, we are sensitive to phase transitions occurring on a timescale of tens of picoseconds. On this timescale we observe a first order metal–insulator transition which probes the kinetics by which a solid phase emerges upon rapid solidification of ejected liquid droplets. We adopt the following procedure to estimate the degree of undercooling associated with the observed rapid solidification. First we assume an initial lattice temperature ranging from 1–5 eV (we estimate the initial lattice temperature at 2 eV). Next we perform calculations for a series of possible solidification temperatures determining, for each, the fraction of probe-region atoms passing through the candidate solidification temperature in 40 ps. If too few ($\ll 1/e^2$) or too many (~ 1) probe-region atoms passes through the candidate solidification temperature in 40 ps then this candidate temperature is rejected. The solidification temperature is taken as that temperature through which $1/e^2$ of the probe-region atoms pass in the measured 40 ps solidification time. Figure 2 shows that the estimated solidification temperatures are 850 K, 1440 K, 1950 K, 2460 K, 2900 K for initial lattice temperatures ranging from 1–5 eV respectively. Accordingly, the initial lattice temperature must be below 3 eV in order to produce an ejecta temperature which is below the melt temperature (1685 K) in 40 ps. Accordingly, hydrodynamic estimates of the undercooling range from $\sim$ 245 K to 835 K for initial lattice temperatures of 2 eV and 1 eV respectively.

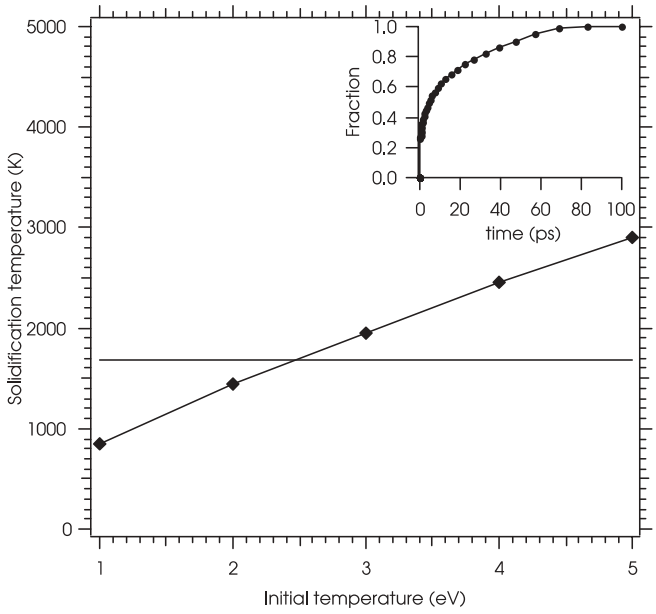

FIGURE 2 Estimated solidification temperature as a function of initial lattice temperature. Solidification temperature is estimated as the temperature through which $1/e^2$ of the probe-region atoms pass during the measured solidification time of 40 ps. The *inset* shows the time-dependent fraction of probe-region atoms passing through 1440 K, the estimated transition temperature corresponding to an initial lattice temperature of 2 eV. The evolution of the system is calculated using the hydrodynamic model discussed in the text

Nucleation rate estimate of undercooling. Finally, we estimate the degree of undercooling using nucleation theory. The nucleation rate is known to depend exponentially on the degree of undercooling and Turnbull (quenching silicon at ~ 10 K/s) obtained a maximum undercooling of $\sim$ 240 °C with an associated (solidification) nucleation rate of $\sim 10^4$ /cm^3 s [25]. At this low nucleation rate less than one critical nucleus would be produced within our probe region in 50 ps indicating that rapid cooling accompanying vacuum expansion leads to significantly enhanced undercooling compared to that obtained in quasi-static experiments. Quantitatively, the observation of solidification in $\sim$ 40 ps is associated with a nucleation rate (R) of $R \sim 10^{30}$ s cc given an estimated probe volume of 1 nm^3 and $\sim$ 1 nm as the size of a critical nucleus. We next estimate the degree of undercooling associated with this nucleation rate.

From classical nucleation theory [20], the nucleation rate (R) can be written as:

$$R = A \exp[-W/KT] \tag{1}$$

$$W = (16\pi/3)(T/\Delta T)^2\eta \tag{2}$$

$$\eta = (\gamma^3/H^2) \tag{3}$$

where A is a (weakly temperature dependent) constant typically ranging from 10^{35}–10^{40} cc s [20], T is the temperature, ΔT specifies the amount temperature T is below the melt temperature, γ is the surface tension (e.g. J/m^2), and H is the heat of fusion (e.g. J/m^3). We calculate a range of nucleation

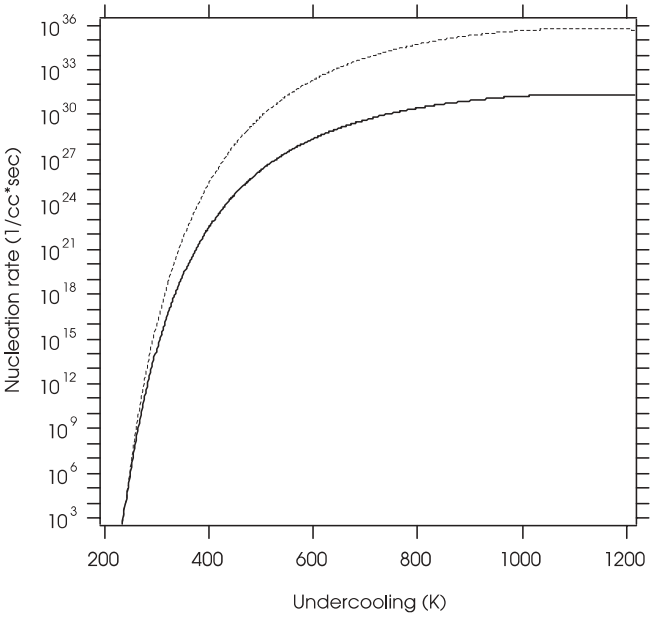

FIGURE 3 (Solidification) Nucleation rate as a function of undercooling as predicted by classical nucleation theory (see text, (1)–(3)). *Dashed curve* $A = 10^{40}$ cc s, $\eta = 0.0125$ eV; *solid curve* $A = 10^{35}$ cc s, $\eta = 0.01076$ eV. 'A' is a numerical prefactor while η is the ratio of the surface tension cubed to the heat of fusion squared (see text)

rates by considering two values of A ($A_1 = 10^{35}$ cc s and $A_2 = 10^{40}$ cc s) and determining the value of η which yields the nucleation rate measured by Turnbull (10^4 cc s at 240 °C undercooling). The associated values of η are $\eta_1 = 0.01076$ eV and $\eta_2 = 0.01250$ eV. These values can be compared with a direct calculation of η (0.138 eV) from (3) given the surface tension (0.73 J/m^2 [8]) and heat of fusion (4.194×10^9 J/m^3 [8]) of silicon. The direct calculation of η is approximately an order of magnitude larger than the value(s) necessary to obtain Turnbull's nucleation rate and adjustment of the constant A over a reasonable range cannot correct for this discrepancy. We note, however, that the values $\eta_{1,2}$ can be obtained with either a factor of 2 decrease in γ, or a factor of 3 increase in H, or correspondingly more modest adjustments to γ and H. Such adjustments are not unreasonable since (1)–(3) are approximate expressions neglecting, for instance, strain energy associated with changes in volume during phase change [20]. More refined expression for the nucleation rate are complex and beyond the scope of the present work. For instance, the calculation of strain energy has been carried out for only a few elementary geometries with many simplifying assumptions [20]. Putting aside a priori estimates of η, the variation of nucleation rate with undercooling as calculated from (1) indicates (Fig. 3) a nucleation rate of $\sim 10^{30}$ cc s for undercooling in the range $\sim$ 500 K–740 K. This range is more restrictive than the range (< 835 K) obtained from hydrodynamic simulations and further suggests that the rapid cooling associated with vacuum expansion leads to significantly enhanced undercooling compared to what has been obtained more conventional quench techniques [25].

5 Summary and conclusions

In summary, the current experiments demonstrate an ability to probe transient material states and metal–insulator transitions occurring early in the vacuum expansion of an extreme material. Solidification is observed to occur rapidly (< 50 ps) following laser excitation, indicating that extreme undercooling drives simultaneous solidification over an appreciable fraction of the ejected fluid volume and that enhanced undercooling can be obtained by vacuum ejection. This may prove useful in attempts to trap potentially novel material states associated with extreme laser heating. Finally, the spectra suggest a low fraction of ejected vapor particles, indicating that semiconductor microparticles do not arise via aggregation of a dilute vapor phase. Instead, we reason that strain associated with gradients in the local expansion velocity leads to fragmentation of the ejecta and an associated particle-size-distribution.

ACKNOWLEDGEMENTS This work was supported by the U.S. Department of Energy under contract AC03-76SF00098.

REFERENCES

1 H.W. Kroto, J.R. Heath, S.C. O'Brien, R.F. Curl, R.E. Smalley: Nature **318**, 162 (1985)
2 A.M. Morales, C.M. Lieber: Science **279**, 208 (1998).
3 P.E. Dyer, S. Farrar, P.H. Key: Appl. Phys. Lett. **60**, 1890 (1992)
4 T.E. Glover: J. Opt. Soc. Am. B **20**, 125 (2003)
5 M. Campagna, R. Rosei: *Photoemission and Absorption Spectroscopy of Solids and Interfaces with Synchrotron Radiation* (North-Holland, Amsterdam, 1990)
6 S. Laville, F. Vidal, T.W. Johnston, O. Barthelemy, M. Chaker, B. Le Drogoff, J. Margot, M. Sabsabi: Phys. Rev. E **66**, 066415 (2002)
7 T.E. Glover, G.D. Ackerman, P.A. Heimann, Z. Hussain, R.W. Lee, H.A. Padmore, C. Ray, R.W. Schoenlein, W.F. Steele, D.A. Young: Phys. Rev. Lett. **90**, 236102 (2003)
8 R.C. Weast, G.L. Tuve (Eds.) *Handbook of Chemistry and Physics* (The Chemical Rubber CO., Ohio, 1972)
9 A. Cavalleri, K. Sokolowski-Tinten, J. Bialkowski, M. Schreiner, D. Von Der Linde: J. Appl. Phys. **85**, 3301 (1999)
10 C. Li, K. Lu, Y. Wang, K. Tamura, S. Hosokawa, M. Inui: Phys. Rev. B **59**, 1571 (1999)
11 V.M. Glazov, S.N. Chizhevskaya, N.N. Glagoleva: *Liquid Semiconductors* (Plenum Press, New York, 1969)
12 J.W. Gadzuk: Phys. Rev. B **14**, 2267 (1976)
13 F. Bechstedt, R. Enderlein: Phys. Stat. Sol. (B) **94**, 239 (1979)
14 F.G. Allen, G.W. Gobeli: Phys. Rev. **127**, 150 (1962)
15 F. Bechstedt, R. Enderlein, R. Fellenberg, P. Streubel, A. Meisel: J. Electron. Spectros. Relat. Phenom. **31**, 131 (1983)
16 P. Baeri, S.U. Campisano, G. Foti, E. Rimini: J. Appl. Phys. **50**, 788 (1979).
17 T. Ohyanagi, A. Miyashita, K. Murakami, O. Yoda: Jpn. J. Appl. Phys. **33**, 2586 (1994)
18 B.L. Holian, D.E. Grady: Phys. Rev. Lett. **60**, 1355 (1988)
19 D. Perez, L.J. Laurent: Phys. Rev. Lett. **89**, 255504 (2002)
20 R.H. Doremus: *Rates of Phase Transformations* (Academic Press Inc., Orlando, 1985)
21 P.H. Bucksbaum, J. Boker: Phys. Rev. Lett. **53**, 182 (1984)
22 R. Kelly, A. Miotello: Applied Surface Science **96–98**, 205 (1996)
23 L.D. Landau, E.M. Lifshitz: *Fluid Mechanics: Landau and Lifshitz Course of Theoretical Physics* Vol. 6 (Butterworth Heinemann, Oxford, 2000)
24 D.A. Young, E.M. Corey: J. Appl. Phys. **78**, 3748 (1995)
25 G. Devaud, D. Turnbull: Appl. Phys. Lett. **46**, 844 (1985)